DALTON

$Na_7Fe_4(PO_4)_6$: a mixed-valence iron phosphate containing a tetramer of edge-sharing FeO_6 octahedra

Kwang-Hwa Lii

Institute of Chemistry, Academia Sinica, Taipei, Taiwan, Republic of China

A novel mixed-valence iron phosphate, $Na_7Fe_4(PO_4)_6$, has been synthesized by a high-temperature, high-pressure hydrothermal method and characterized by single-crystal X-ray diffraction and Mössbauer spectroscopy. The compound crystallizes in the trigonal space group $R\bar{3}c$ with $a = 13.392(2)$, $c = 17.858(3)$ Å, $U = 2773.7(8)$ Å^3, $Z = 6$ and $R = 0.0179$. The structure consists of tetrameric units of edge-sharing FeO_6 octahedra, which are connected by corner-sharing PO_4 tetrahedra to form a three-dimensional framework structure, enclosing a network of cavities where the sodium cations reside. Mössbauer spectroscopy supports the presence of one Fe^{II} and three Fe^{III} in a tetrameric unit.

Iron phosphates exist as minerals and have a rich crystal chemistry. These minerals are often basic and/or hydrated phosphates and are among the most perplexing substances in the mineral kingdom, as indicated by Moore.[1] The structures of many of these iron phosphates consist of clusters or aggregates of iron–oxygen polyhedra as basic building units. For example, an octahedral tetramer forms the basis for leucophosphite,[2] a face-sharing cluster of three octahedra for rockbridgeite and dufrenite,[1] a nonameric ring of edge-sharing octahedra for mitridatite,[3] an infinite corner-sharing chain for laueite[4] and an infinite edge-sharing chain for alluaudite.[5] Although a large number of possible clusters can be constructed from iron–oxygen polyhedra, iron phosphate minerals seem to favour only a very small number of them. The structures of most phosphates are highly polymerized, being dominated by frameworks and sheets.

In nature many minerals crystallize from hot, water-rich solutions. By using autoclaves, hydrothermal growth in the laboratory closely duplicates the natural process. For example, crystals of leucophosphite, $KFe_2(PO_4)_2(OH)(H_2O)\cdot H_2O$,[6] and a triclinic polymorph of sincosite, $Ca(VO)_2(PO_4)_2\cdot 4H_2O$,[7] have been synthesized. A number of synthetic iron phosphates have also been synthesized by the hydrothermal technique, *viz.* $AFeP_2O_7$ (A = Rb or Cs),[8] $SrFe_3(PO_4)_3(HPO_4)$,[9] $AFe_3(P_2O_7)_2$ (A = Sr or Ba),[10] $AFe_5(PO_4)_5(OH)\cdot H_2O$ (A = Ca or Sr),[11] $CaFe_2(PO_4)_2(HPO_4)$,[12] $RbFe(HPO_4)_2$,[13] $CsFe_3(PO_4)_3(H_2O)_2$,[14] $CaFe_3(PO_4)_3(H_2O)$[15] and $K_3Fe_3(PO_4)_4\cdot 2H_2O$.[16] Their structures contain FeO_6 octahedra, FeO_5 trigonal bipyramids, dimers of corner-sharing, edge-sharing or face-sharing FeO_6 octahedra, trimeric units of Fe–O polyhedra, and infinite chains of FeO_6 octahedra sharing edges and corners. They include iron(II), iron(III) and mixed-valence compounds, with several containing diphosphate groups. To our knowledge, face-sharing octahedral dimers and diphosphate groups do not occur in any iron phosphate minerals. There is a greater variety of clusters in these synthetic compounds than in the minerals. These interesting compounds present a challenge to complete structural characterization in terms of basic research.

In this paper, the synthesis, crystal structure, and Mössbauer spectroscopy of a novel iron phosphate, $Na_7Fe_4(PO_4)_6$, is reported. This phosphate contains mixed-valence iron atoms and its structure consists of a tetrameric unit of edge-sharing FeO_6 octahedra.

Experimental

Synthesis

High-temperature, high-pressure hydrothermal syntheses were performed in gold ampoules contained in a Leco Tem-Pres autoclave where pressure was provided by water pumped by a compressed air-driven intensifier. The phosphate, $Na_7Fe_4(PO_4)_6$, was initially synthesized by heating a mixture of $Na_2HPO_4\cdot 2H_2O$ (0.1424 g), $NaH_2PO_4\cdot H_2O$ (0.2208 g), Fe_2O_3 (0.0639 g) and H_2O (0.6 cm^3) (Na:P:Fe molar ratio = 4:3:1) to 550 °C. The mixture was soaked at this temperature for 8 h, achieving a pressure of 38 000 lbf in^{-2} (*ca.* 262 × 10^6 Pa). The autoclave was then cooled to 250 °C at 5 °C h^{-1} and quenched to ambient temperature by removing the autoclave from the furnace. The product was filtered off, washed with water, rinsed with ethanol and dried in a desiccator at ambient temperature. The product contained dark green crystals of $Na_7Fe_4(PO_4)_6$, a colourless solid and a small amount of red solid. Suitable dark green crystals were obtained which allowed the determination of the structure by X-ray diffraction. The colourless and red solids were not characterized because of poor crystal quality or insufficient amount of sample. The dark green colour is indicative of mixed valence and it is worthy of note that Fe_2O_3 was the only source of iron in the reaction mixture. Under these hydrothermal conditions, hydrogen could be formed by the reaction of water with the steel wall of the autoclave. Its slow diffusion through the gold ampoule led to partial reduction of Fe^{3+} to Fe^{2+}. Subsequently, hydrothermal treatment of $Na_2HPO_4\cdot 2H_2O$ (0.2854 g), $NaH_2PO_4\cdot H_2O$ (1.1061 g) (molar ratio Na:P = 1.167), Fe_2O_3 (0.2422 g), Fe (0.0154 g) and H_2O (2.6 cm^3) in a gold ampoule (8 × 0.9 cm inside diameter) under the same reaction conditions gave dark green crystals of $Na_7Fe_4(PO_4)_6$ as the major product and a very small amount of a black needle-like material. The black needles were intimately mixed with the dark green crystals such that hand sorting of enough pure sample for spectroscopy measurements was not possible. The yield was about 95% based on iron. Powder X-ray diffraction using a MAC Science diffractometer on the bulk product was performed. The product was nearly a single phase of $Na_7Fe_4(PO_4)_6$. The intensity of the most intense reflection of the impurity ($d = 3.13$ Å) was 6% of that of the major phase, and all other observed reflections in the diffraction pattern

were in excellent agreement with those in a calculated powder pattern. The sample was used for Mössbauer spectroscopy measurements (see below).

Mössbauer spectroscopy

The ^{57}Fe Mössbauer measurements were made on a constant-acceleration instrument at room temperature. Velocity calibrations were made using 99.99% pure 10 μm iron foil. Typical linewidths for all three pairs of iron lines fell in the range 0.28–0.30 μm s^{-1}. Isomer shifts are reported with respect to iron foil at 300 K. It should be noted that the isomer shifts illustrated are plotted as experimentally obtained; tabulated data should be consulted.

Single-crystal X-ray diffraction

A dark green crystal of dimensions 0.18 × 0.12 × 0.12 mm was used for indexing and intensity data collection on an Enraf-Nonius CAD4 diffractometer with κ-axis geometry using monochromated Mo-Kα radiation. Unit-cell parameters were determined by a least-squares fit of 25 peak maxima having $26 < 2\theta < 35°$. Three standard reflections were measured every 2 h (no decay). Axial oscillation photographs were taken to check the cell parameters. Of the 1088 reflections collected ($2\theta_{max} = 50°$, scan mode 2θ–θ), 486 reflections were considered observed [$I > 2.5\sigma(I)$] after Lorentz polarization and empirical absorption correction ($R_{int} = 0.015$). Corrections for absorption were based on ψ scans of several suitable reflections with χ values close to 90° using the NRCVAX program package.[17] On the basis of systematic absences, statistical analysis of the intensity distribution, and successful solution and refinement of the structure, the space group was determined to be $R\bar{3}c$ (no. 167). The structure was solved by direct methods and successive Fourier syntheses, and was refined by full-matrix least-squares refinement based on F values. The Na(2) atom was located at 6b special positions, Fe(1) at 6a, Fe(2) at 18e, and all other atoms at 36f general positions. The occupancy factor of each metal atom was allowed to refine but in no case deviated significantly from full occupancy. The final cycle of full-matrix least-squares refinement including atomic coordinates and anisotropic thermal parameters converged at $R = 0.0179$ and $R' = 0.0184$. The final difference electron density map was featureless and the highest peak and deepest hole were 0.30 and −0.32 e Å^{-3}, respectively. Neutral-atom scattering factors for all atoms were used. Anomalous dispersion and secondary extinction corrections were applied. Structure solution and refinement were performed on a VAX computer system using the SHELXTL PLUS programs.[18]

Complete atomic coordinates, thermal parameters and bond lengths and angles have been deposited at the Cambridge Crystallographic Data Centre. See Instructions for Authors, *J. Chem. Soc., Dalton Trans.*, 1996, Issue 1.

Results and Discussion

Structure

The crystallographic data are listed in Table 1, atomic coordinates in Table 2 and interatomic distances, bond angles and bond-valence sums[19] in Table 3. Atom Na(2) is located at $\bar{3}$ (special positions 6b), Fe(1) has a local symmetry of 32 (6a), Fe(2) sits on a two-fold axis (18e), and all other atoms are at general positions. The Fe and P atoms are six- and four-co-ordinated, respectively.

The phosphate, $Na_7Fe_4(PO_4)_6$, adopts a new type of structure and its framework is formed of FeO_6 octahedra and PO_4 tetrahedra, as illustrated in the polyhedral view parallel to the [001] direction in Fig. 1. The basic building unit of the framework is shown in Fig. 2 to consist of four FeO_6 octahedra and six PO_4 tetrahedra. The central Fe(1)O_6 octahedron shares its three skew edges with three Fe(2)O_6 octahedra. The point-group symmetry of each building unit is D_3. Alternatively, the building unit can be described as a cubic close-packed array of oxygen atoms with the iron and phosphorus atoms at the octahedral and tetrahedral sites, respectively. Each unit is further connected to three units above and three units below to form a three-dimensional framework with large cavities being occupied by Na^+ cations. Each cavity is surrounded by eight building units. Adjacent cavities are interconnected through open windows which are formed by the edges of four octahedra

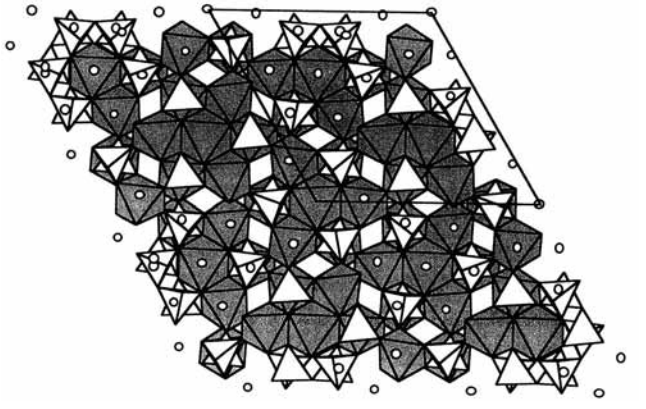

Fig. 1 Polyhedral representation of the $Na_7Fe_4(PO_4)_6$ structure along the [001] direction. Open circles are Na atoms

Table 1 Crystallographic data and details of the structure determination for $Na_7Fe_4(PO_4)_6$

Formula	$Fe_4Na_7O_{24}P_6$
M	954.15
Crystal system	Trigonal
Space group	$R\bar{3}c$
a/Å	13.392(2)
c/Å	17.858(3)
U/Å^3	2773.7(8)
Z	6
D_c/g cm^{-3}	3.427
F(000)	2778
μ(Mo-Kα)/cm^{-1}	39.0
T/°C	23
λ(Mo-Kα)/Å	0.709 30
Scan range/°	0.80 + 0.35 tan θ
Maximum 2θ/°	50
Reflections collected	1088
Unique reflections	547
Observed unique reflections [$I > 2.5\sigma(I)$]	486
$T_{min,max}$	0.8884, 1.0
Number of parameters	65
R^a	0.0179
R'^b	0.0184
Goodness-of-fit	1.524
$(\Delta\rho)_{max,min}$/e Å^{-3}	0.30, −0.32

^{a} $R = \Sigma||F_o| - |F_c||/\Sigma|F_o|$. ^{b} $R' = [\Sigma w(|F_o| - |F_c|)^2/\Sigma w|F_o|^2]^{\frac{1}{2}}$. Weighting scheme, $w^{-1} = \sigma^2(F) + 0.000\,019F^2$; least-squares weights are multiplied by $1 - \exp[-5(\sin\theta/\lambda)^2]$.

Table 2 Atomic coordinates for $Na_7Fe_4(PO_4)_6$

Atom	x	y	z
Na(1)	0.685 6(1)	0.126 3(1)	0.277 72(8)
Na(2)	0	0	0.5
Fe(1)	0.666 67	0.333 33	0.083 33
Fe(2)	0.666 67	0.114 76(4)	0.083 33
P(1)	0.814 71(5)	0.010 37(6)	0.356 06(4)
O(1)	0.851 4(1)	−0.067 6(2)	0.313 2(1)
O(2)	0.682 8(2)	−0.044 1(2)	0.346 1(1)
O(3)	0.851 7(2)	0.015 9(2)	0.436 2(1)
O(4)	0.869 3(2)	0.132 2(2)	0.321 1(1)

Table 3 Interatomic distances (Å), bond angles (°) and bond-valence sums (Σs) for $Na_7Fe_4(PO_4)_6$

$Fe(1)O_6$ octahedron *

Fe(1)	O(1a)	O(1b)	O(1c)	O(1d)	O(1e)	O(1f)
O(1a)	**2.063(2)**	2.990(3)	2.990(3)	2.939(4)	2.749(4)	
O(1b)	92.9(1)	**2.063(2)**	2.990(3)	2.749(4)		2.939(4)
O(1c)	92.9(1)	92.9(1)	**2.063(2)**		2.939(4)	2.749(4)
O(1d)	90.9(1)	83.6(1)	175.0(1)	**2.063(2)**	2.990(3)	2.990(3)
O(1e)	83.6(1)	175.0(1)	90.9(1)	92.9(1)	**2.063(2)**	2.990(3)
O(1f)	175.0(1)	90.8(1)	83.6(1)	92.9(1)	92.9(1)	**2.063(2)**

Σs[Fe(1)–O] = 2.47

$Fe(2)O_6$ octahedron *

Fe(2)	O(1c)	O(1e)	O(2a)	O(2b)	O(4a)	O(4b)
O(1c)	**2.085(1)**	2.939(4)	2.842(2)		2.735(3)	2.742(3)
O(1e)	89.6(1)	**2.085(1)**		2.842(2)	2.742(3)	2.735(3)
O(2a)	88.8(1)	172.0(1)	**1.974(2)**	2.881(4)	2.751(3)	3.119(3)
O(2b)	172.0(1)	88.8(1)	93.7(1)	**1.974(2)**	3.119(3)	2.751(3)
O(4a)	84.1(1)	84.4(1)	87.7(1)	103.5(1)	**1.997(2)**	
O(4b)	84.4(1)	84.1(1)	103.5(1)	87.7(1)	163.7(1)	**1.997(2)**

Σs[Fe(2)–O] = 3.00

$P(1)O_4$ tetrahedron

P(1)	O(1)	O(2)	O(3)	O(4)
O(1)	**1.558(3)**	2.499(3)	2.463(3)	2.567(3)
O(2)	107.2(1)	**1.548(2)**	2.555(3)	2.473(2)
O(3)	107.1(1)	113.7(1)	**1.504(2)**	2.516(3)
O(4)	111.5(1)	106.1(1)	111.2(1)	**1.546(2)**

Σs[P(1)–O] = 4.95

Na(1)–O(1)	2.848(2)	Na(1)–O(2)	2.572(3)
Na(1)–O(2)	2.649(3)	Na(1)–O(3)	2.281(2)
Na(1)–O(3)	2.629(2)	Na(1)–O(3)	2.579(2)
Na(1)–O(4)	2.543(3)	Na(1)–O(4)	2.815(2)

Σs[Na(1)–O] = 0.99

Na(2)–O(3) 2.390(2) (× 6)

Σs[Na(2)–O] = 1.23

* The distances between the *trans* oxygen atoms are not shown.

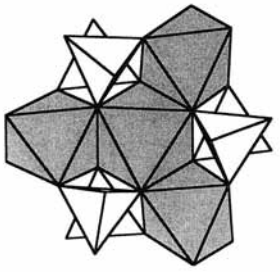

Fig. 2 Basic building unit in the $Na_7Fe_4(PO_4)_6$ structure viewed along [001]. The central $Fe(1)O_6$ octahedron shares its three skew edges with three $Fe(2)O_6$ octahedra

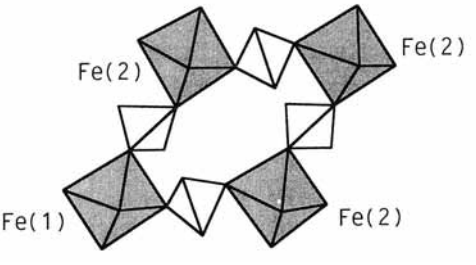

Fig. 3 Open window connecting adjacent cavities in the $Na_7Fe_4(PO_4)_6$ structure viewed along [2$\bar{2}$1]

and four tetrahedra (Fig. 3). The shortest oxygen–oxygen distance across the window is 4.58 Å, which is smaller than twice the sum of the radii for $^{VI}Na^+$ (1.02 Å) and $^{IV}O^{2-}$ (1.38 Å). The window is not open enough for easy ion passage. Each phosphate group makes three P–O–Fe links and one terminal link, which partakes in Na–O bonds. The $Fe(2)O_6$ octahedron is strongly distorted because of edge-sharing, as indicated by the Fe(2)–O and O • • • O distances in Table 3. The Fe(2)–O bonds involving the edge-sharing oxygen, O(1), are the longest. The $Fe(1)O_6$ octahedron is considerably more regular. Atom Fe(2) is displaced from the centroid of its Fe–O octahedron away from Fe(1) by 0.138 Å, whereas Fe(1) is at the centroid of its octahedron. The common edges are 2.939 Å and are considerably longer than most of the edges which are not shared. In many oxide, silicate and phosphate minerals containing edge-sharing polyhedra, the two oxygen atoms forming a common edge draw closer together to shield better the positive charges on metal cations. Conversely, the shared edges in $Na_7Fe_4(PO_4)_6$ do not shorten. Atoms O(1), which form the shared edges, are each shared by a PO_4 group which also bridges over adjacent Fe(2) within the same building unit, and consequently the O(1) atoms are restrained from approaching each other. The PO_4 tetrahedron is also strongly distorted, as indicated from the P–O and O • • • O distances. The four P–O bond distances can be divided into two groups: three long distances at 1.546–1.558 Å and a short one at 1.504 Å. The short P–O bond involves the oxygen atom which co-ordinates to Na^+ cations only. The longest O • • • O distance in a PO_4 tetrahedron involves two O atoms which are bonded to Fe atoms within the same building unit.

The co-ordination number of each Na atom was determined on the basis of the maximum gap in the Na–O distances ranked

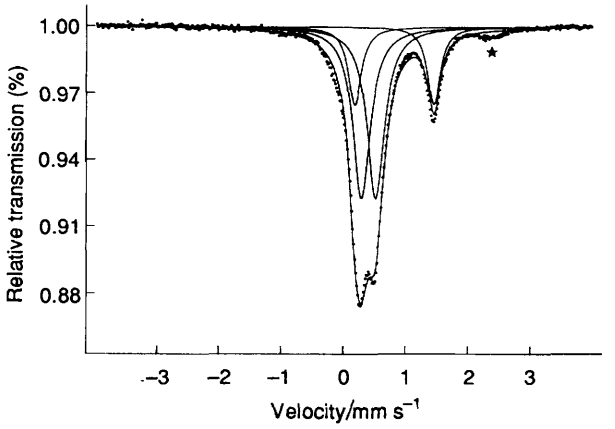

Fig. 4 Mössbauer spectrum of $Na_7Fe_4(PO_4)_6$ at 300 K. The peak indicated with an asterisk is attributed to an impurity phase

Table 4 Mössbauer spectral parameters (mm s^{-1}) for $Na_7Fe_4(PO_4)_6$ at 300 K

	Intensity ratio	δ^a	$\Delta E_Q{}^b$	Γ^c
Component 1	1	0.91	1.27	0.25, 0.25
Component 2	3	0.50	0.23	0.34, 0.34

[a] Isomer shift (referred to iron). [b] Quadrupole splitting. [c] Full width at half-height.

in increasing order. The maximum cation–anion distance, L_{max}, according to Donnay and Allmann,[20] was also considered. Therefore, Na(1) and Na(2) are co-ordinated by eight and six oxygen atoms with the ninth Na(1)–O and seventh Na(2)–O distances at 3.055 and 3.756 Å, respectively. The geometry of Na(1)–O polyhedra appears irregular. The Na(2) atom is at the centroid of a distorted octahedron. The valence sum for Na(1) is in good agreement with its formal oxidation state. The valence sum for Na(2) indicates that it is more tightly bound, which is consistent with its smaller thermal parameters. The Fe(2) atom is trivalent, as indicated from the result of the bond-valence calculation; Fe(1) has to be divalent in order to balance the charge. However, the calculation result for Fe(1) is inconclusive. Contrary to this, the assessed valence sums of the Fe atoms in all the iron(II) or mixed-valence iron phosphates that we have recently synthesized are in good agreement with their formal charges. The Fe(1) atom appears more tightly bound to oxygen atoms than Fe(2), as is inferred from a comparison of their thermal parameters. The space available for Fe(1) is very confined because of the six bridging phosphate tetrahedra. Consequently, the Fe(1)–O bond is shorter than the average Fe^{2+}–O bond length. The presence of one Fe^{II} and three Fe^{III} is confirmed by Mössbauer spectroscopy.

Mössbauer spectroscopy

As shown in Fig. 4, the room-temperature Mössbauer spectrum of $Na_7Fe_4(PO_4)_6$ was least-squares fitted with two doublets with a constraint on the area ratio of 1 : 3. The area and half-width of the high- and low-velocity components of the quadrupole doublets were constrained to be equal. All the spectral parameters are listed in Table 4. Component 1 has an isomer shift characteristic of Fe^{III} and can be assigned to Fe(2). Component 2 has an isomer shift typical of Fe^{II} and can be assigned to Fe(1). The small peak indicated with an asterisk is attributed to the impurity phase. The isomer shifts for both components 1 and 2 are consistent with those for high-spin Fe^{III} and Fe^{II} respectively.[21] The Mössbauer spectrum strongly supports the presence of one Fe^{II} and three Fe^{III} in $Na_7Fe_4(PO_4)_6$. The amount of impurity, as is inferred from a comparison of peak areas, is about 4.5%, which is approximately the same as that estimated from powder X-ray diffraction.

In conclusion, a new mixed-valence iron phosphate, $Na_7Fe_4(PO_4)_6$, has been synthesized and structurally characterized. Its structure consists of a tetrameric cluster which is formed of a central $Fe^{II}O_6$ octahedron sharing its skew edges with three $Fe^{III}O_6$ octahedra. The compound is, to my knowledge, the first phosphate having this type of cluster. The tetramer is completely different from that in leucophosphite, $K_2[Fe^{III}_4(OH)_2(H_2O)_2(PO_4)_4]\cdot 2H_2O$, which consists of an edge-sharing dimer whose two common corners each fuse by corner-sharing to two other octahedra. This new phosphate, $Na_7Fe_4(PO_4)_6$, further expands the variety of structures in the iron phosphate phase space which contain clusters of Fe–O polyhedra linked *via* phosphate tetrahedra. Explorations of the M–Fe–P–O phase space using the high-temperature, high-pressure hydrothermal technique are continuing in an effort to prepare other new phases containing novel clusters of Fe–O polyhedra.

Acknowledgements

Support for this study by the Institute of Chemistry, Academia Sinica and the National Science Council (NSC 84-2113-M-001-006) is acknowledged. The author thanks Professor T.-Y. Dong at National Sun Yat-Sen University for Mössbauer spectroscopy measurements.

References

1 P. B. Moore, *Am. Mineral.*, 1970, **55**, 135.
2 P. B. Moore, *Am. Mineral.*, 1972, **57**, 397.
3 P. B. Moore and T. Araki, *Inorg. Chem.*, 1977, **6**, 1096.
4 P. B. Moore, *Am. Mineral.*, 1965, **50**, 1884.
5 P. B. Moore, *Am. Mineral.*, 1971, **56**, 1955.
6 L.-S. Wu and K.-H. Lii, unpublished work.
7 H.-Y. Kang, W.-C. Lee, S.-L. Wang and K.-H. Lii, *Inorg. Chem.*, 1992, **31**, 4743.
8 E. Dvoncova and K.-H. Lii, *J. Solid State Chem.*, 1993, **105**, 279.
9 K.-H. Lii, T.-Y. Dong, C.-Y. Cheng and S.-L. Wang, *J. Chem. Soc., Dalton Trans.*, 1993, 577.
10 K.-H. Lii, P.-F. Shih and T.-M. Chen, *Inorg. Chem.*, 1993, **32**, 4373.
11 E. Dvoncova and K.-H. Lii, *Inorg. Chem.*, 1993, **32**, 4368.
12 K.-H. Lii, *J. Chem. Soc., Dalton Trans.*, 1994, 931.
13 K.-H. Lii and L.-S. Wu, *J. Chem. Soc., Dalton Trans.*, 1994, 1577.
14 K.-H. Lii and C.-Y. Huang, *J. Chem. Soc., Dalton Trans.*, 1995, 571.
15 K.-H. Lii and C.-Y. Huang, *Eur. J. Solid State Inorg. Chem.*, 1995, **32**, 225.
16 K.-H. Lii, *Eur. J. Solid State Inorg. Chem.*, 1995, **32**, 746.
17 E. J. Gabe, Y. Le Page, J. P. Charland and F. L. Lee, *J. Appl. Crystallogr.*, 1989, **22**, 384.
18 G. M. Sheldrick, SHELXTL PLUS Crystallographic System, Release 4.11, Siemens Analytical X-Ray Instruments Inc., Madison, WI, 1990.
19 I. D. Brown and D. Altermatt, *Acta Crystallogr., Sect. B*, 1985, **41**, 244.
20 G. Donnay and R. Allmann, *Am. Mineral.*, 1970, **55**, 1003.
21 F. C. Hawthorn, in *Reviews in Mineralogy*, ed. F. C. Hawthorn, Mineralogical Society of America, Washington, 1988, vol. 18, pp. 255–340.

Received 8th September 1995; *Paper* 5/05951H